Urban Monitoring by 4D Change Detection Using Multi-temporal SAR Images

CHIA-HSIANG YANG[1] & UWE SOERGEL[1]

Zusammenfassung: Die wachsende Bevölkerung und der Trend zur Urbanisierung haben viele bauliche Veränderungen in Städten zur Folge. Deren Erkennung und Überwachung ist essentiell für Zwecke wie kommunale Verwaltung, Stadtplanung oder Katasterfortführung. Konventionelle Vermessungen vor Ort sind zwar sehr genau, jedoch aufwendig und können nur punktuell durchgeführt werden. Im Gegensatz dazu ist mit Fernerkundung eine kostengünstige und großflächige Datengewinnung möglich. Moderne SAR-Satelliten sind in der Lage, hochaufgelöste Radarbilder in dichtem zeitlichen Raster zu erfassen. Aktives SAR hat zudem den Vorteil der Allwetterfähigkeit und der Nachtsicht, weshalb sich SAR insbesondere für auf Zeitreihen von Bildern basierende Überwachungsaufgaben eignet. Multitemporale SAR-Bilder werden daher häufig zu Zwecken der Änderungsdetektion ausgewertet. Wir stellen ein neu entwickeltes Verfahren zur 4D-Änderungserkennung vor, womit gemeint ist, dass sowohl räumliche (3D) als auch zeitliche (1D) Änderungen erkannt werden können. Dieses Verfahren wird anhand von SAR-Bildstapeln demonstriert, die den Innenstadtbereich von Berlin abdecken. Insbesondere liegt das Augenmerk auf der Erkennung von Baumaßnahmen, in deren Zuge alte Gebäude abgerissen oder neue errichtet werden.

Abstract: The continuous rise in population and economic growth has led to frequent urban changes such as construction. Monitoring such changes is important for city management, urban planning, updating of cadastral maps, etc. In contrast to conventional field surveys, which are usually expensive and slow, remote sensing techniques are fast and cost-effective alternatives. Spaceborne synthetic aperture radar (SAR) provides radar images captured rapidly over vast areas at fine spatiotemporal resolution. In addition, the active microwave sensors are capable of day-and-night vision and independent of weather conditions. The advantages mentioned above make SAR suitable for monitoring tasks. Change detection approaches based on multi-temporal SAR images are widely used for urban monitoring. We developed a novel 4D change detection technique, which is capable of detecting spatial changes (3D) and occurrence times (1D). In this study, we apply our technique to a built-up area in the centre of Berlin, Germany. As a result, the disappearing and emerging structures along with their occurrence times are successfully detected. We have demonstrated that these spatiotemporal results are able to provide detailed and comprehensive information for urban monitoring.

1 Introduction

Human activities, such as population growth, economic globalization, urban extension, and natural disasters have led to frequent urban changes. Monitoring such changes is important for city management, urban planning, updating of cadastral map, environmental monitoring, disaster assessment, etc. (GAMBA 2013; MARIN et al. 2015). In contrast to conventional field surveys, which are usually expensive and slow, remote sensing techniques are fast and cost-effective

[1] Universität Stuttgart, Institut für Photogrammetrie, Geschwister-Scholl-Str. 24D, D-70174 Stuttgart,
E-Mail: [chia-hsiang.yang, uwe.soergel]@ifp.uni-stuttgart.de

alternatives. Spaceborne synthetic aperture radar (SAR) provides radar images captured rapidly over vast areas at fine spatiotemporal resolution. In addition, the active microwave sensors are capable of day-and-night vision and independent of weather conditions. The advantages mentioned above make SAR suitable for monitoring tasks.

Time series analysis based on SAR images is widely used for urban monitoring. Among them, persistent scatterer interferometry (PSI) (CROSETTO et al. 2016; FERRETTI et al. 2000, 2001, 2011; HOOPER et al. 2004; KAMPES 2006) detects and analyses PS points, which are characterized by strong, stable, and coherent radar signals throughout a SAR image stack and can be regarded as substructures in human settlements. Attributes of PS points, including line-of-sight velocities (mm/year level), topography heights, geographic positions, etc., can be derived and used for monitoring of structural deformation and 3D modelling. A prerequisite of forming PS points is that their signals must maintain temporal coherence. For example, to avoid coherence loss, buildings covered with PS-like substructures must be steady and free of any big changes during an entire acquisition period of SAR images. In contrast, if the substructures disappear or emerge arbitrarily due to construction, the corresponding temporary PS points are discarded at the initial screening of temporally stable scatterers in a standard PSI processing.

Certain approaches (BRCIC & ADAM 2013; FERRETTI et al. 2003; NOVALI et al. 2004; YANG et al. 2016) are dedicated to retrieve temporary PS points, which exist in a portion of time-series SAR images due to big changes. Among them, our previous work (YANG et al. 2016) proposed "4D Change Detection Based on PSI" (4DCDPSI) to recognizes two types of temporary PS points subject to big changes, which are called disappearing big change (DBC) and emerging big change (EBC) points, along with their occurrence times. This technique has been validated by the simulated and real data tests.

In this paper, we apply our 4D change detection technique to the centre of Berlin, Germany to explore the applications of monitoring construction progress, business districts, sports playgrounds, traffic infrastructures, and single buildings. We first introduce PSI and 4DCDPSI in Sections 2 and 3, respectively. Section 4 demonstrates the spatiotemporal changes over the entire study area, followed by the in-depth discussions on five zoom-in areas with respect to different applications. Finally, the conclusions are summarized in Section 5.

2 Persistent Scatterer Interferometry

A time series of N complex SAR images, which are acquired from the same orbit and cover a common extent, is required as input data. Among the series, slave images are precisely co-registered to a master image, which is selected under small baseline constraint (BERARDINO et al. 2002; LANARI et al. 2004). Then, N-1 interferograms between the master and all of the slave images are computed. The interferometric phases of each pixel are used to estimate its temporal coherence, line-of-sight velocity, and relative topography height via a Periodogram process (FERRETTI et al. 2001). A temporal coherence serves as a measure of phase stability throughout the SAR image stack. Finally, pixels with high temporal coherences are selected as PS points. However, DBC and EBC points, if any, are just discarded as they suffer coherence loss during the entire SAR image sequence. To retrieve such big change information, we resort to the 4D change detection technique described in the next section.

3 4D Change Detection Based on Persistent Scatterer Interferometry

We first illustrate the change detection scheme subject to a single break date that big changes occur before or after. Complete, front, and back SAR image sets are defined from an image sequence for use in this scheme. The complete set consists of all of the images in the sequence. The front and back sets comprise the images taken before and after a specified break date, respectively. Our aim is to find PS points that exist in the front set but disappear in the back set and vice versa. The PS points that suddenly disappear are termed DBC points and those emerging in the back set are called EBC points.

The flowchart of single-break-date change detection (Fig. 1) is composed of the persistence, disappearance, and emergence scenarios, in which the complete, front, and back sets are mainly involved, respectively. These three image sets are processed by a standard PSI procedure to generate three temporal coherence images. We suppose that the temporal coherence of a DBC or EBC point in the front or back set is higher than that in the complete set, which is reduced due to the big change. Based on this assumption, the change indices of each pixel x in the disappearance (CI^{D}) and emergence (CI^{E}) scenarios are calculated by

$$\underset{[-1\,,\,+1]\in\mathrm{R}}{CI^{\mathrm{D}}(x)} = \gamma_{\mathrm{T}}^{\mathrm{F}}(x) - \gamma_{\mathrm{T}}^{\mathrm{C}}(x) \quad (1)$$

$$\underset{[-1\,,\,+1]\in\mathrm{R}}{CI^{\mathrm{E}}(x)} = \gamma_{\mathrm{T}}^{\mathrm{B}}(x) - \gamma_{\mathrm{T}}^{\mathrm{C}}(x) \quad (2)$$

where $\gamma_{\mathrm{T}}^{\mathrm{C}}$, $\gamma_{\mathrm{T}}^{\mathrm{F}}$, and $\gamma_{\mathrm{T}}^{\mathrm{B}}$ denote the temporal coherences in the complete, front, and back sets. A pixel is more likely to be a DBC or EBC point when CI^{D} and CI^{E} is closer to 1, respectively. A change index distribution over DBC or EBC points is modelled to be a right-tailed probability function towards 1. Then, a statistical-based thresholding is applied to the change indices of the pixels to extract DBC and EBC points. The extracted points are jointly analysed with the PS points, which are selected in the persistence scenario, to reject two types of outliers. First, PS points are discarded if they coincide with the other two point labels. Second, a DBC point must not be an EBC point as well and vice versa. The remaining pixels without any label are regarded as undefined (U) points. Finally, the PS, DBC, and EBC points are combined into a change detection result. However, the accurate times of big changes are lacking as they are only known to disappear and emerge after and before the break date, respectively.

To detect accurate big change times, a set of single-break-date results are jointly analysed in a multi-break-date change detection (Fig. 2). For each pixel, two sequences, i.e., change indices and initial point labels (PS, DBC, EBC, or U), have been determined thus far. Some of the initial labels may be erroneous due to processing uncertainty in each single-break-date change detection. The majority vote is then applied to each label sequence to determine the pixel' label, e.g., a pixel is labelled PS if most of its initial labels are PS. Nevertheless, false labels are still unavoidable but can be removed by an outlier filtering. Three outlier types are described below along with their removal strategies using sliding window operation.

- Homogeneous points are expected to form a single object. For example, PS points are unlikely to appear on a demolished apartment full of DBC points. For this reason, PS, DBC, or BC points, which are in the majority in a window, are retained; the other inconsistent points are then deleted.

- An isolated PS, DBC, or EBC point in a window is removed considering that its reliability cannot be inspected by comparing with neighbours.
- A PS point is removed if its velocity is too large or quite different from the velocities of the neighbouring PS points in a window.

Once the PS, DBC, and EBC points are confirmed, the remaining points are considered to be U points. Then, the change date of each DBC or EBC point is detected from the time-series break dates based on the temporal variation in its change index sequence. The concept is to detect the turning point of a change index sequence, which corresponds to a disappearance or emergence date. In the end, the PS, DBC, and EBC points along with the change dates are combined to illustrate the spatiotemporal changes.

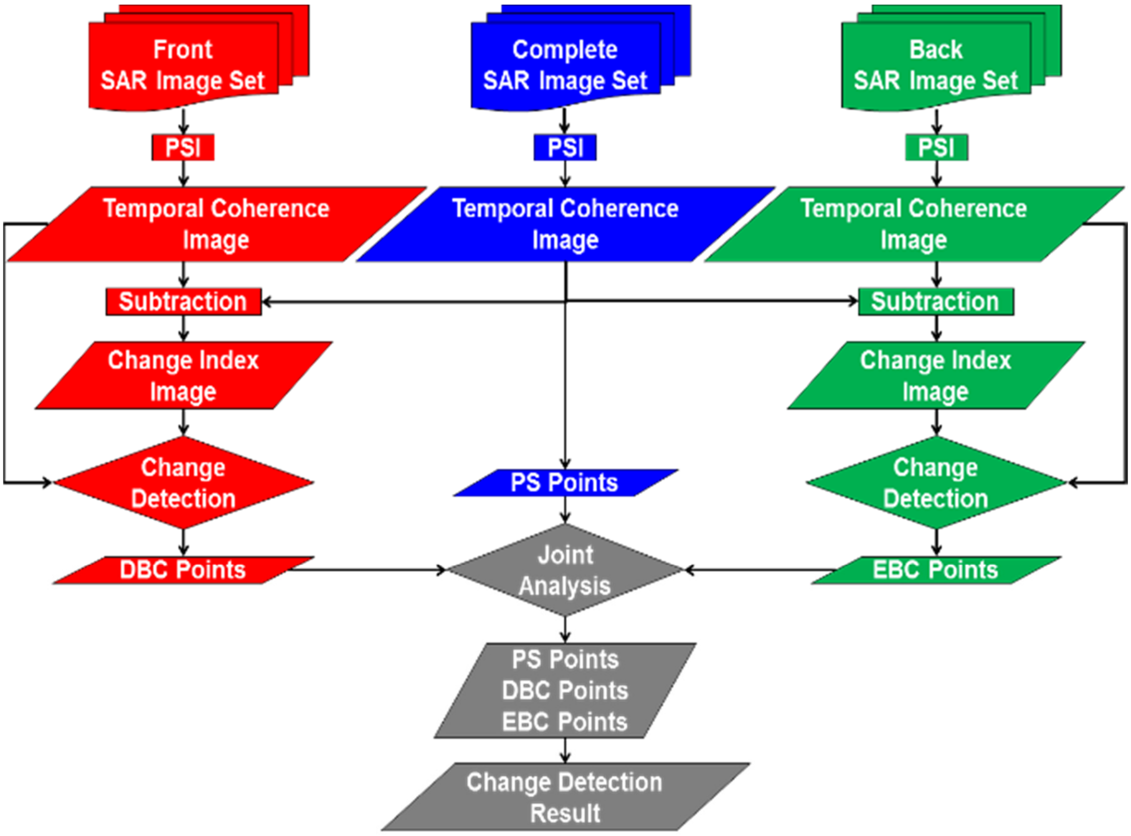

Fig. 1: Flowchart of single-break-date change detection. Persistence (blue), disappearance (red), and emergence (green) scenarios are dedicated to extracting PS, DBC, and EBC points, respectively (YANG et al. 2016)

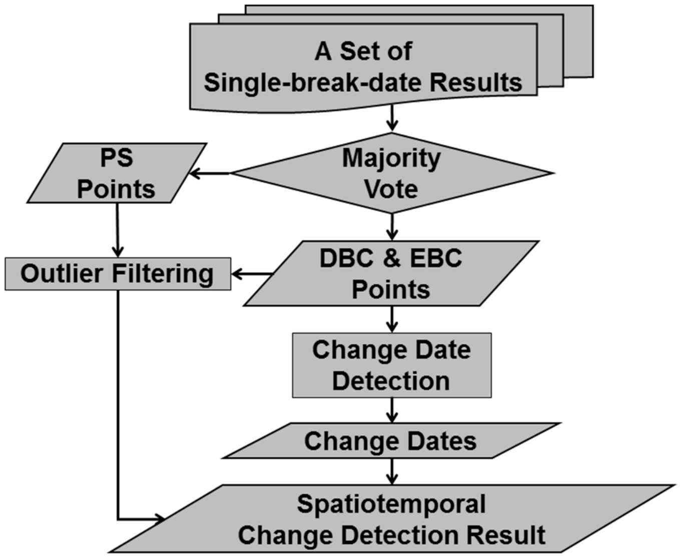

Fig. 2: Flowchart of multi-break-date change detection. (YANG et al. 2016)

4 Real Data Test

In this test, we adopted forty TerraSAR-X (TSX) images acquired in High Resolution Spotlight mode from October 27, 2010 to September 4, 2014. Thirteen break dates are set during 2013, i.e., we conducted thirteen single-break-date instances, which were jointly processed by multi-break-date change detection. All of the images are precisely co-registered and resampled into 5000 × 5000 with ground resolution of 1 m, which is able to represent detailed substructures. The study area (Fig. 3) covering the city centre in Berlin, Germany shows many bright clusters of strong signals on structures that appear to be potential PS points. Two Google Earth (GE) images (ground truth) taken on September 12, 2010 and September 5, 2014 reveal that many building constructions occurred within the image acquisition period and are thus good examples for comparison with our test result. The spatiotemporal changes (Fig. 4) show where and when the structures disappeared and emerged. We focus our following discussions on the patches 1 to 5 for different applications of urban monitoring.

We first explore the construction events around Berlin Central Station (Fig. 5). The office complex of Federal Ministry of the Interior (area 1) had been constructed in the second half of 2013. A series of construction events is present in area 2. The quad-square structures were removed at the early stage. The upper-left hotel had been erected over time by 2013; another hotel and two office buildings cannot be detected because the constructions were still in progress. Certain new surface substructures in areas 3, 4, and 7 are able to be detected by our method; in contrast, these substructures are hardly identified from the GE images. Another construction event, which is also difficult to be recognized from the GE images, is illustrated in area 5 where the bridge was renovated during a couple of early months in 2013. Area 6 displays two new office buildings that were constructed at different schedules. The right building had been completed earlier, giving rise to a building-shaped pattern formed by clustered EBC points. In contrast, the construction progress on the left building was slower as only sparse EBC points appeared in late 2013.

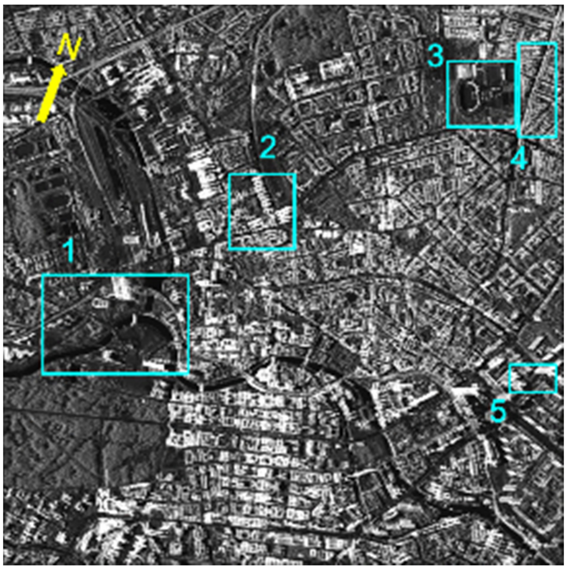

Fig. 3: Mean TSX image over study area. Patches 1 to 5 are used for in-depth analysis

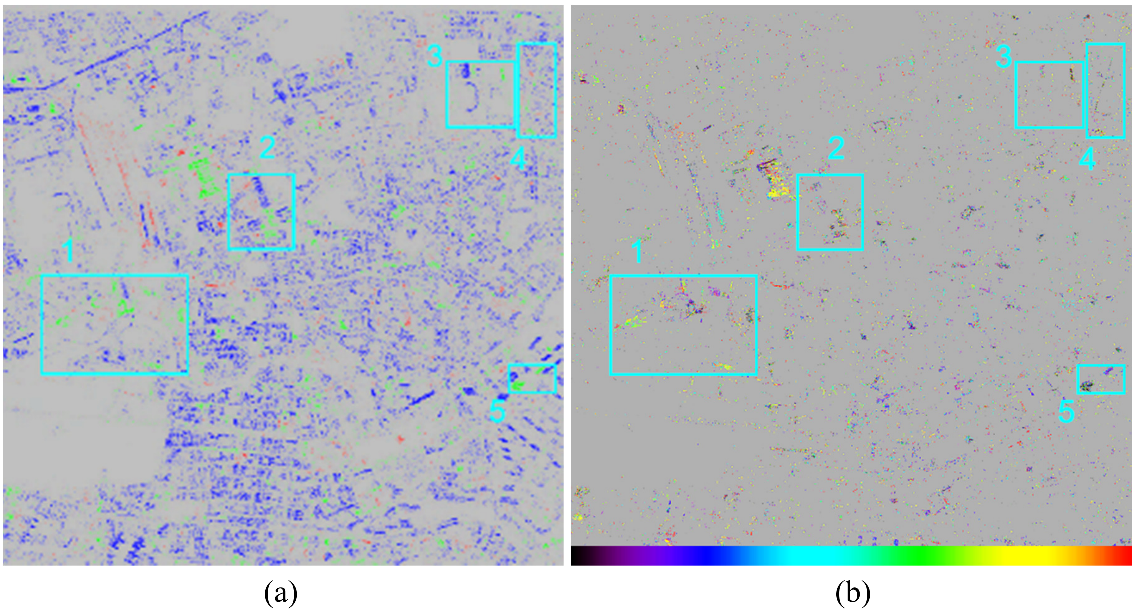

Fig. 4: Spatiotemporal change detection result. Patches 1 to 5 are used for in-depth analysis. (a) Steady, disappearing, and emerging structures represented by PS (blue, 41277/km^2), DBC (red, 2200/km^2), and EBC (green, 7180/km^2) points. (b) Disappearance and emergence dates: black to red, earliest to latest in 2013.

The second example (Fig. 6) is about monitoring a business district, in which building changes are usually frequent and need cost-effective surveillance schemes. In the early 2013, the buildings in areas 1 and 2 were demolished; and the main structures of the new buildings appeared in areas 3 to 7 and their constructions continued to the end of 2013. Since the second half of 2013, certain substructures had been added to the German Railway's office complex in area 8. These additions seem vague in the GE images but are clearly revealed in the spatiotemporal change detection result.

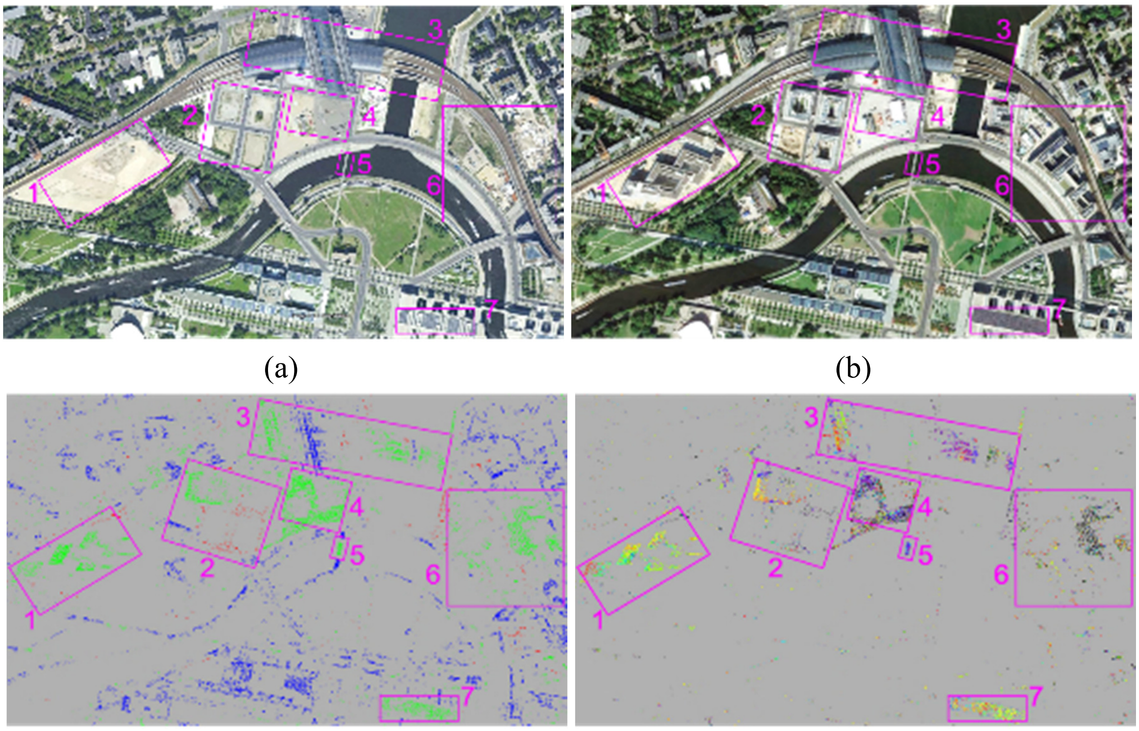

(a) (b)

(c) (d)

Fig. 5: Construction monitoring in patch 1 (Fig. 3) around Berlin Central Station. Areas 1 to 7 are used for in-depth analysis. GE images were acquired on (a) September 12, 2010 and (b) September 5, 2014. (c) and (d): spatiotemporal change detection result in patch 1 (Fig. 4).

Monitoring sports facilities is demanded for citizen safety. In case of structural damages, DBC points might be found at certain times. In Olympiastadion Berlin (Fig. 7), two detected change events include a structural renovation (area 1) on the upper-left arena and an erection of a new building (area 2) beside a sports playground. Most importantly, the upper-left arena and lower-left stadium seem steady without structural damages as the intensive PS points are found on them rather than DBC points. If necessary, the line-of-sight velocities of the PS points can be utilized for investigation on structural deformation.

Traffic infrastructure monitoring is useful for transportation management especially in busy cities and extending human settlements. For example, our technique detects a new elevated metro line across a couple of blocks that was under construction in 2013 (Fig. 8). The main structure had been accomplished in the early dates, followed by some partial substructures.

The last example demonstrates construction monitoring of single high-rise buildings (Fig. 9). The left building's main structure (area 1) had been erected in early 2013 and the remaining substructures were later complemented over time. In area 2, certain new storeys were built upon an existing building from low to high level in sequence along the magenta arrow (Fig. 9(d)).

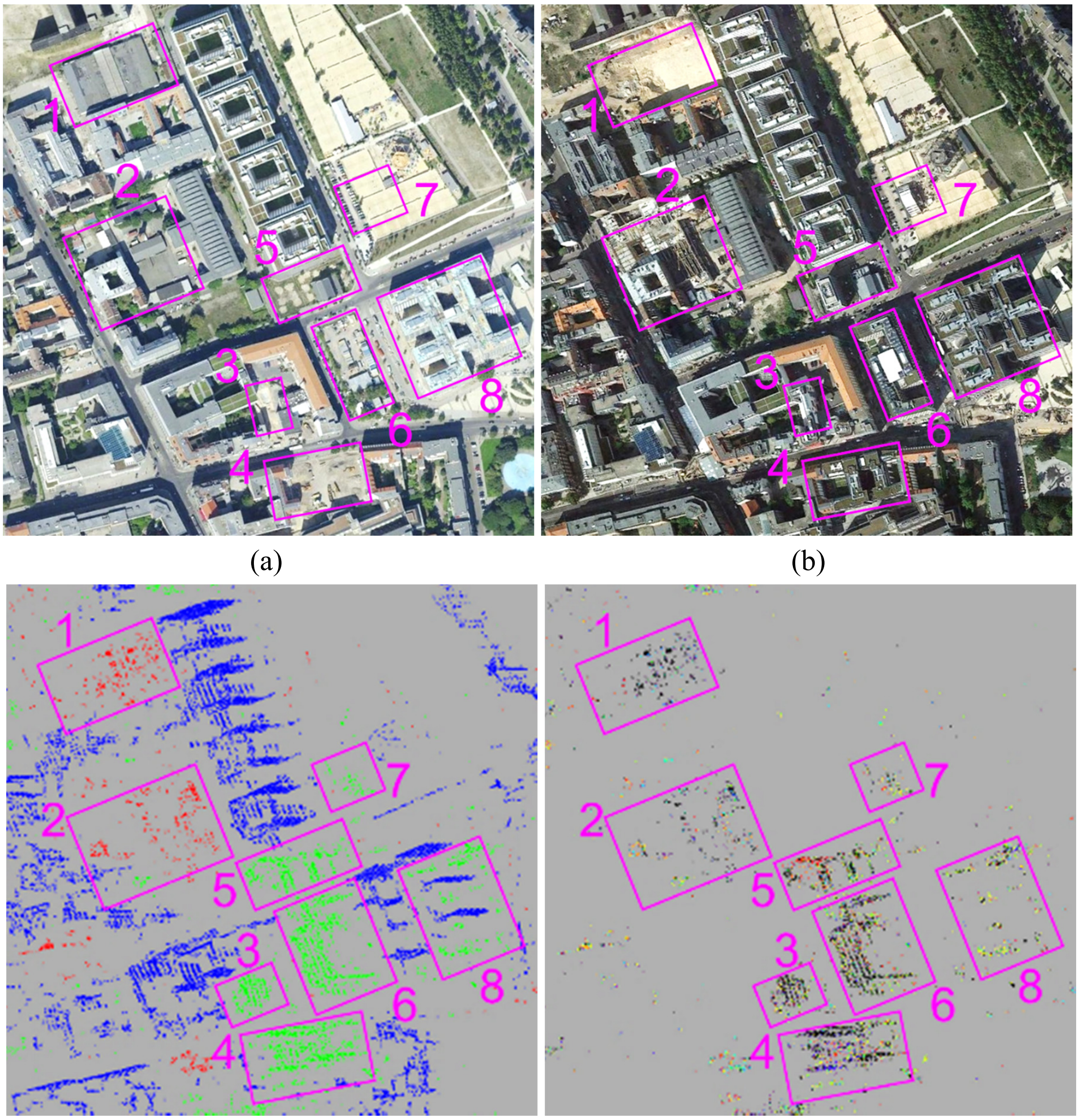

(a) (b) (c) (d)

Fig. 6: Business district monitoring in patch 2 (Fig. 3). Areas 1 to 8 are used for in-depth analysis. GE images were acquired on (a) September 12, 2010 and (b) September 5, 2014. (c) and (d): spatiotemporal change detection result in patch 2 (Fig. 4).

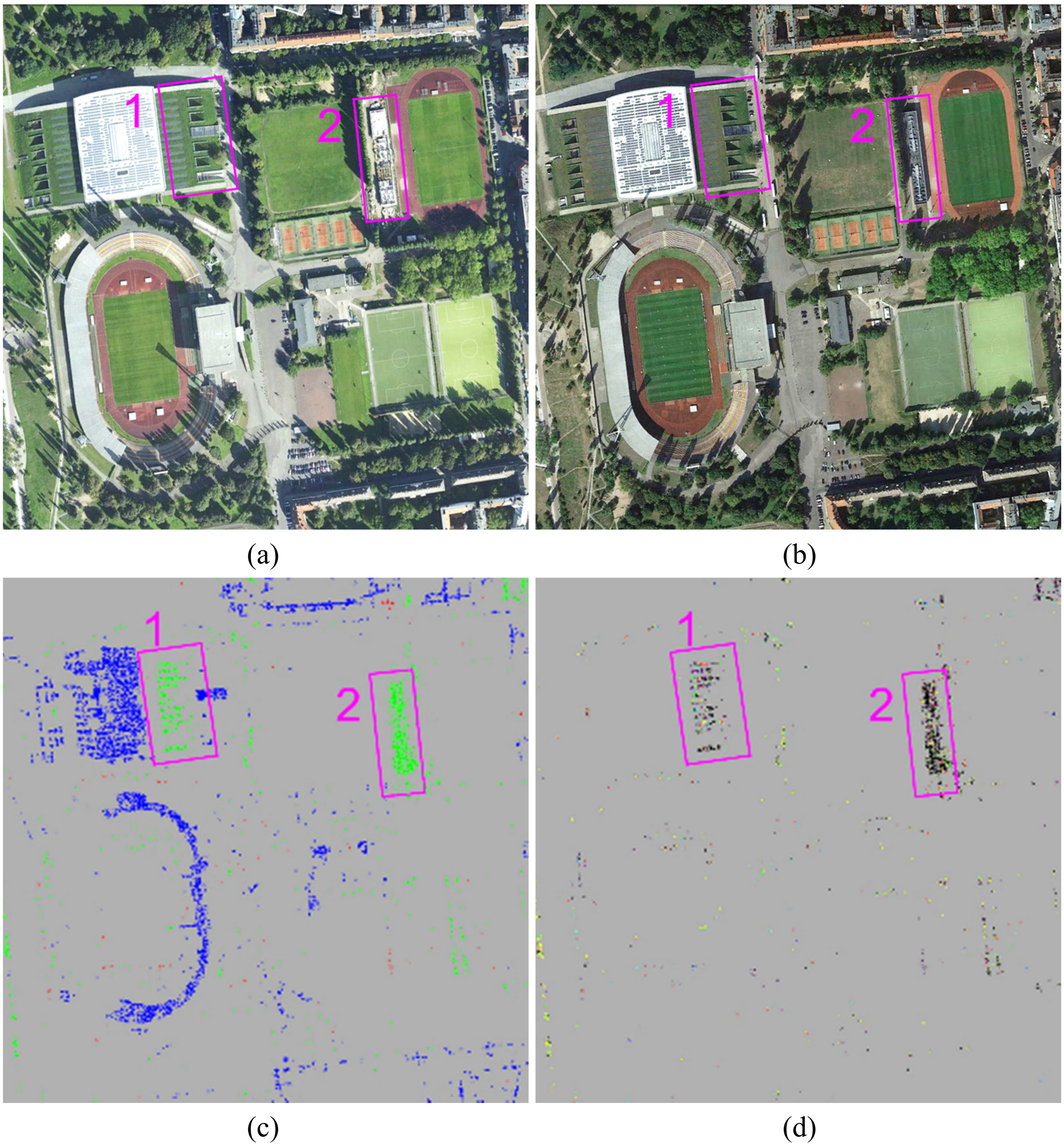

Fig. 7: Sports facility monitoring in patch 3 (Fig. 3). Areas 1 to 2 are used for in-depth analysis. GE images were acquired on (a) September 12, 2010 and (b) September 5, 2014. (c) and (d): spatiotemporal change detection result in patch 3 (Fig. 4).

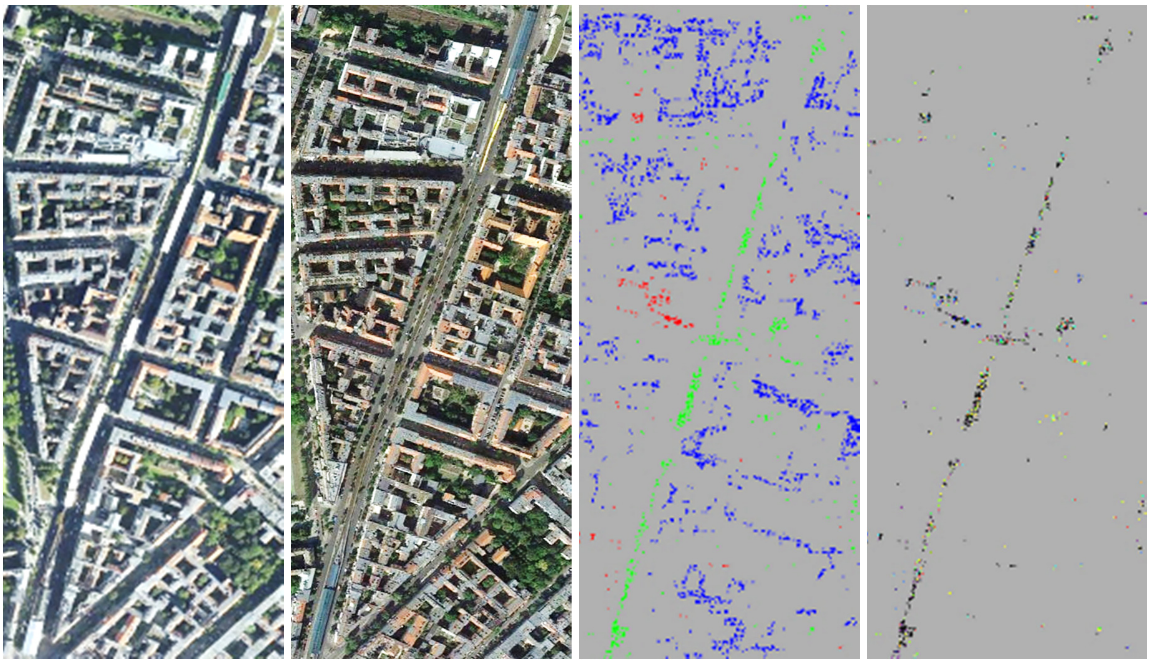

(a) (b) (c) (d)

Fig. 8: Traffic infrastructure monitoring in patch 4 (Fig. 3). GE images were acquired on (a) September 12, 2010 and (b) September 5, 2014. (c) and (d): spatiotemporal change detection result in patch 4 (Fig. 4).

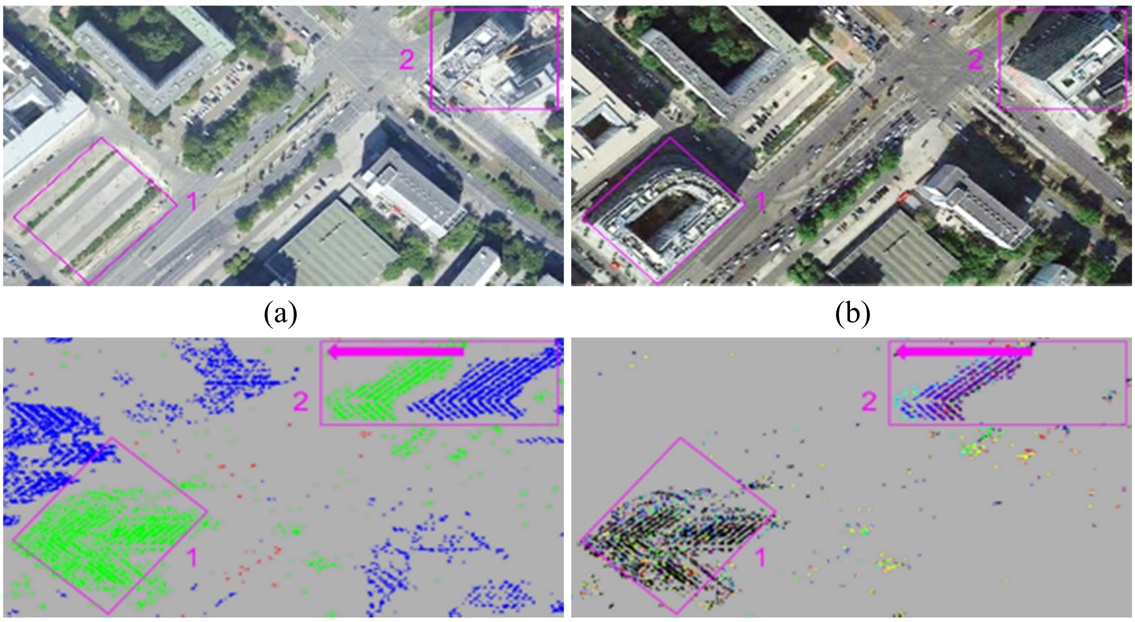

(a) (b)

(c) (d)

Fig. 9: Construction monitoring of single high-rise buildings in patch 5 (Fig. 3). Areas 1 to 2 are used for in-depth analysis. GE images were acquired on (a) September 12, 2010 and (b) September 5, 2014. (c) and (d): spatiotemporal change detection result in patch 5 (Fig. 4).

5 Conclusions

A novel time series analysis, 4DCDPSI, has been proven capable of detecting spatial changes (3D) and occurrence times (1D). In this study, we explore the feasibility and applicability of 4DCDPSI for urban monitoring. The aims of the five case studies are to monitor construction progress, business districts, sports facilities, traffic infrastructures, and single buildings. As to construction monitoring, three main construction types, i.e., demolition, erection, and renovation, can be distinctly recognized along with change times that substructures are added or removed. Such spatiotemporal change information is able to be derived from a business district characterized by frequent and intensive building changes. Our method can also provide detailed construction progress on single buildings. A typical example in our case studies detects some new storeys that were built upon an existing high-rise building form low to high level in sequence. In addition to building construction, we also demonstrate that construction monitoring of traffic infrastructures is also feasible by bringing an example of a newly-built elevated metro line. Last but not least, fortunately, we only find dense PS points instead of DBC points, which are regarded as structural damages, on the sports facilities. In summary, we have demonstrated that our technique can provide detailed and comprehensive information for urban monitoring.

6 Literatures

BERARDINO, P., FORNARO, G., LANARI, R. & SANSOSTI, E., 2002: A New Algorithm for Surface Deformation Monitoring Based on Small Baseline Differential SAR Interferogram. IEEE Transactions on Geoscience and Remote Sensing **40**(11), 2375-2382.

BRCIC, R. & ADAM, N., 2013: Detecting Changes in Persistent Scatterers. Proceedings of IEEE IGARSS, Melbourne, Australia, 117-120.

CROSETTO, M., MONSERRAT, O., CUEVAS-GONZÁLEZ, M., DEVANTHÉRY, N. & CRIPPA, B., 2016: Persistent Scatterer Interferometry: A Review. ISPRS Journal of Photogrammetry and Remote Sensing **115**, 78-89.

FERRETTI, A., PRATI, C. & ROCCA, F., 2000: Nonlinear Subsidence Rate Estimation Using Permanent Scatterers in Differential SAR Interferometry. IEEE Transactions on Geoscience and Remote Sensing **38**(5), 2202-2212.

FERRETTI, A., PRATI, C. & ROCCA, F., 2001: Permanent Scatterers in SAR Interferometry. IEEE Transactions on Geoscience and Remote Sensing **39**(1), 8-20.

FERRETTI, A., COLESANTI, C., PERISSIN, D., PRATI, C. & ROCCA, F., 2003: Evaluating The Effect of The Observation Time on The Distribution of SAR Permanent Scatterers. Proceedings of FRINGE, Frascati, Italy.

FERRETTI, A., FUMAGALLI, A., NOVALI, A., PRATI, C., ROCCA, F. & RUCCI, A., 2011: A New Algorithm for Processing Interferometric Data-stacks: SqueeSAR. IEEE Transactions on Geoscience and Remote Sensing **49**(9), 3460-3470.

GAMBA, P., 2013: Human Settlements: A Global Challenge for EO Data Processing and Interpretation. Proceedings of the IEEE **101**(3), 570-581.

HOOPER, A., ZEBKER, H., SEGALL, P. & KAMPES, B., 2004: A New Method for Measuring Deformation on Volcanoes and Other Natural Terrains Using InSAR Persistent Scatterers. Geophysical Research Letters **31**(23), 1-5.

KAMPES, B. M., 2006: Radar Interferometry: Persistent Scatterer Technique. Springer.

LANARI, R., MORA, O., MANUNTA, M., MALLORQUÍ, J. J., BERARDINO, P. & SANSOSTI, E., 2004: A Small Baseline Approach for Investigating Deformations on Full Resolution Differential SAR Interferograms. IEEE Transactions on Geoscience and Remote Sensing **42**(7), 1377-1386.

MARIN, C., BOVOLO, F. & BRUZZONE, L., 2015: Building Change Detection in Multitemporal Very High Resolution SAR Images. IEEE Transactions on Geoscience and Remote Sensing **53**(5), 2664-2682.

Novali, F., Basilico, M., Ferretti, A., Prati, C. & Rocca, F., 2004: Advances in Permanent Scatterer Analysis: Semi and Temporary PS. Proceedings of EUSAR, Berlin, Germany.

YANG, C., KENDUIYWO, B. K. & SOERGEL, U., 2016: 4D Change Detection Based on Persistent Scatterer Interferometry. Proceedings of ICPR&PRRS, Cancun, Mexico.